Kinetic Analysis of Cyclophilin-Catalyzed Prolyl *Cis/Trans* Isomerization by Dynamic NMR Spectroscopy†

Dorothee Kern, Gunther Kern,‡ Gerd Scherer, Gunter Fischer,* and Torbjörn Drakenberg§

Arbeitsgruppe "Enzymologie der Peptidbindung", Max-Planck-Gesellschaft zur Förderung der Wissenschaften e.V., Weinbergweg 16A, D-06120 Halle/Saale, Germany

Received May 15, 1995; Revised Manuscript Received July 31, 1995⊗

ABSTRACT: To investigate the kinetics of the prolyl peptide bond *cis/trans* isomerization of *N*-succinyl-Ala-Phe-Pro-Phe-(4-)nitroanilide catalyzed by peptidyl prolyl *cis/trans* isomerases (PPIases), one-dimensional dynamic ^{1}H NMR spectroscopy was employed. To this end line shape analyses of proton signals were performed at various concentrations of both cytosolic porcine kidney cyclophilin (Cyp18) and peptide substrate. Catalysis of the *cis/trans* isomerization by Cyp18 is best described by a four-site exchange model, where the four sites represent the *cis* and *trans* isomers free in solution and bound to the enzyme. Combination of dynamic NMR spectroscopy with the classical protease-coupled PPIase assay allowed determination of the complete set of the microscopic rate constants describing the four site exchange model. The comparison of the rate constants of *cis* → *trans* isomerization of the peptide free in solution and bound to cyclophilin yields an acceleration factor of 3.5×10^5. Dissociation of the Michaelis complexes are of the same order of magnitude as the isomerization rates on the enzyme. Therefore, all microscopic rate constants contribute to the steady state parameters. For the first time, the k_{cat} (620 s^{-1}) and K_M (220 μM) value for the *trans* isomer in addition to the values of the *cis* isomer (k_{cat} = 680 s^{-1}, K_M = 80 μM) could be determined under reversible conditions at pH 6.0 and 10 °C. The affinity of Cyp18 for the *cis* isomer is 4 times higher than for the *trans* isomer. This results in a shift of the *cis/trans* equilibrium toward the *cis* isomer. The 1.8 ppm downfield chemical shift of the *cis* signal of the substrate amide proton of Phe^5 could be explained by hydrogen bonding of the *cis* peptide unit to the enzyme. This might be the reason for the preferred binding of the *cis* isomer. Finally, the results suggest that during catalysis the residues N-terminal to proline remain fixed to Cyp18 while the C-terminal part is rotated.

The *cis/trans* isomerization of prolyl peptide bonds often determines the overall rate in protein folding (Schmid et al., 1993). The ubiquitously distributed peptidyl prolyl *cis/trans* isomerases (PPIase,[1] EC 5.2.1.8) catalyze the *cis/trans* isomerization in short peptides (Fischer et al., 1984) and proteins *in vitro* (Bächinger, 1987; Lang et al., 1987; Lang & Schmid, 1988; Lin et al., 1988; Schönbrunner et al., 1991; Mücke & Schmid, 1992; Fransson et al., 1992; Kern et al., 1995). Only a few *in vivo* examples for PPIase-mediated protein folding exist so far (Steinmann et al., 1991; Lodish & Kong, 1991; Ondek et al., 1992; Baker et al., 1994). The interest in PPIase was further raised by the identification of the PPIases as the binding proteins for the immunosuppressive drugs cyclosporin A (CsA) (Fischer et al., 1989a; Takahashi et al., 1989) and FK506 (Harding et al., 1989; Siekierka et al., 1989). PPIases have been detected in virtually all cellular compartments and organisms (Fischer, 1994). They are classified due to their specific binding and inhibition by the immunosuppressive drugs CsA and FK506 in cyclophilins and FKBPs, respectively.

Despite lacking information about biological consequences of catalysis, a number of cellular binding proteins for PPIases could be characterized (Nadeau et al., 1993; Friedman at al., 1993; Johnson & Toft, 1994; Cardenas et al., 1994) which may include putative natural substrates. Recently, human cyclophilin A was reported to be essential for formation of infectious human immunodeficiency virus (Franke et al., 1994; Thall et al., 1994).

Selective inhibition of the different PPIases in the cell may provide information about their role *in vivo*. For a rational design of inhibitors, it is necessary to understand the mechanism of PPIase catalysis. Previous experiments to determine the kinetic parameters of PPIase catalysis are based on coupling of the reversible *cis/trans* isomerization to an irreversible reaction. In protein refolding, the irreversible reaction comprises the formation of thermodynamically stabilized *cis* or *trans* conformation in the native state (Schmid et al., 1993). In the case of isomer-specific proteolysis of substrates of the type Xaa-Pro-Yaa-(4-)-nitroanilide, the irreversible step is represented by the proteolytic cleavage of the 4-nitroanilide when the Xaa−Pro peptide bond is in the *trans* conformation (Fischer et al., 1984). Kofron et al. (1991) improved this photometric assay and determined the K_M and k_{cat} values for the *cis* isomer. This coupled irreversible assay has several limitations: (1) only chromogenic peptides with the Xaa-Pro-

† The work was supported by the Studienstiftung des Deutschen Volkes, the Deutsche Forschungsgemeinschaft (Fi 455/1-3), the Boehringer-Ingelheim Stiftung, and the Swedish National Science Research Council.

* To whom correspondence should be addressed.

‡ Present address: Institut für Biochemie/Biotechnologie, Abt. Enzymologie, Martin-Luther Universität, Weinbergweg 16A, D-06120 Halle/Saale, Germany.

§ Permanent address: Department of Physical Chemistry 2, Chemical Center, University of Lund, Box 124, S-22100 Lund, Sweden and Chemical Technology, The Technical Research Centre of Finland, Box 1401, FIN-02044 VTT, Finland.

⊗ Abstract published in *Advance ACS Abstracts,* September 15, 1995.

[1] Abbreviations: CsA, cyclosporin A; DMSO, dimethyl sulfoxide; FID, free induction decay; FKBP, FK506 binding protein; NMR, nuclear magnetic resonance; PPIase, peptidyl prolyl *cis/trans* isomerase; (4-)NA, 4-nitroanilide; Suc, succinyl; TRNOE, transferred nuclear Overhauser enhancement; 1D, one dimensional; 2D, two dimensional.

0006-2960/95/0434-13594$09.00/0

Phe-(4-) nitroanilide sequence can be analyzed (using other proteases it is possible to investigate sequences with amino acids other than Phe), (2) the kinetic analysis is only possible under nonequilibrium conditions, (3) only the *cis* → *trans* and not the reverse *trans* → *cis* reaction can be characterized, (4) proteolytic products or the helper protease could influence the PPIase activity, and (5) the determination of microscopic rate constants is not possible.

Some limitations can be overcome by an uncoupled photometric PPIase assays based on rapid solvent pertubation experiments (Garcia-Echeverria et al., 1992, 1993). However, substrates designed specifically are necessary and time course analysis of the catalyzed reaction may be complicated.

Dynamic NMR spectroscopy is a method to overcome all these limitations. Previous studies have shown that it is possible to investigate the catalysis of *cis/trans* isomerization of peptides by dynamic NMR spectroscopy. In two-dimensional (2D) NMR (Justice et al., 1990; Kern et al., 1993) and saturation transfer experiments (Hsu et al., 1990; London et al., 1990; Videen et al., 1994), only apparent second-order constants for the enzyme catalysis could be determined. However, using line shape analyses, a detailed characterization of the enzyme kinetics is possible. In our previous studies we showed that the enzyme mechanism does not fit a simple two-state mechanism (Hübner et al., 1991). Here we report a complete kinetic analysis of the PPIase catalysis under equilibrium conditions and show that the kinetics can be described by a four-site exchange model, which involves the free and the enzyme-bound forms of the *cis* and *trans* isomers of the peptide. All microscopic rate constants in this model could be determined.

MATERIALS AND METHODS

Enzyme Preparation. The 18 kDa cytosolic cyclophilin (Cyp18)[2] was isolated from porcine kidney as described previously (Fischer et al., 1984). Cyp18 is 98.8% identical to human Cyp18 (Haendler et al., 1987). For the NMR measurements, the protein solution was diafiltrated and concentrated into 10 mM deuterated phosphate buffer, pD 6.4, and stored at 4 °C. The protein concentration was determined by absorbance at 280 nm (ϵ_{280} = 8140 M^{-1} cm^{-1}); the amount of enzymatically active Cyp18 was measured by active site titration with CsA.

NMR Sample Preparation. N-Succinyl-Ala-Phe-Pro-Phe-(4-)nitroanilide (Suc-Ala-Phe-Pro-Phe-(4-)NA) was dissolved in 10 mM phosphate buffer, pH 6.0 (10% D_2O used for the lock signal), to stock solutions of 20 and 40 mM. The total peptide concentration was measured by absorbance at 390 nm after complete cleavage of the 4-nitroanilide residue from the peptide by concentrated NaOH. To a sample (430 μL) of a solution initially containing 400 μM peptide were added six 10 μL aliquots of the Cyp18 stock solution (96 μM), followed by six 20 μL aliquots of this enzyme solution. Subsequently seven 5 μL aliquots of the peptide stock solutions were added to the sample. NMR experiments were performed after each addition.

NMR Measurements. One-dimensional proton NMR experiments (1D ^1H NMR) were performed on a General Electric Omega 500 spectrometer operating at 500.13 MHz and processed on a Sun 3/260 workstation using the Omega software. The spectra were aquired at 10 °C with 64−2000 scans, depending on the sample concentration. A total of 8192 complex data points were used with a spectral width of 6410 Hz. The carrier was set on the solvent resonance, and the water signal was suppressed by presaturation for 3 s; 90° pulses were used with an aquisition time of 1.3 s. The FIDs were multiplied with an exponentional function of 1 Hz line broadening to improve the signal/noise ratio. The spectra were referenced to the water signal [4.92 ppm vs sodium 3-(trimethylsilyl)propionate].

Active Site Titration (Handschumacher et al., 1984). Aliquots of 2.5 μL of a 0.1 mM CsA stock solution in DMSO were added to 800 μL of a 3.6 μM cyclophilin solution (calculated from absorbance at 280 nm). Assuming that the concentration of bound CsA reflects the amount of intact active sites, the increase in fluorescence emission of Cyp18 at 339 nm (exication at 280 nm) due to formation of a 1:1 complex with CsA was measured at 10 °C after 20 min incubation time.

Isomer-Specific Proteolysis (Protease-Coupled PPIase Assay). The assay for determination of the PPIase activity before and after the NMR experiments was performed as previously described (Fischer et al., 1984) with the following alterations. The peptide stock solutions were used as described above; the peptide was preincubated and the reaction was started with chymotrypsin because the diluted NMR samples already contained small amounts of peptide. We ruled out, by applying external Suc-Ala-Ala-Pro-PheO$^-$ (0−2 mM), that in this special case an analogous reaction product of the *trans* isomer cleavage did competitively influence the measured k_{cat}/K_M value at the conditions used.

Since the enzyme concentrations used in the NMR experiments are much higher than in the protease-coupled PPIase assay, and keeping in mind the decameric nature of the Cyp18 in the crystal lattice (Pfügl et al., 1993), it is necessary to sure that the specific enzyme activity is not concentration dependent in the range between 1 nM (this PPIase assay) and 16 μM (highest concentration in the NMR experiments). Using overlapping sets of substrates differing in their k_{cat}/K_M values, the enzyme activity of Cyp18 could be determined from 1 nM to 3 μM enzyme. The activity of Cyp18 varied linearly with the enzyme concentration. Measurements at concentrations above 3 μM Cyp18 were not possible due to the high rate of the catalyzed reaction. However, the linear dependence is valid for 3 orders of magnitude up to concentrations already used in the NMR experiments. Light scattering experiments did not indicate aggregation in the concentration range used. In addition, the structure determination of Cyp18 by NMR spectroscopy was performed at a concentration of 4 mM (Wüthrich et al., 1991) and aggregation at this concentration, 200-fold higher than what we have used, would have made the structure determination impossible.

Line Shape Analyses. The quantum mechanical density matrix formalism was used for the line shape analyses (Sack, 1958; Binsch, 1969; Limbach, 1991). After a pulse creating single-quantum coherence, the time dependence of the density matrix ρ is represented by

$$d\rho/dt = M\rho$$

in the Liouville space (Binsch, 1969). For the description of the A part of an AX spin system, which undergoes exchange between four sites A−D according to Scheme 1, the matrix **M** is the sum of two submatrices M_e given by with $e = \pm 1$ and the population vector $\rho(0) = (p_A, p_B, p_C,$

[2] The abbreviation Cyp18 is used for the 18 kDa cytosolic cyclophilin from porcine kidney.

$$M_e = \begin{bmatrix} -k_{AB} - k_{AD} - R_2^*{}_A + 2\pi i(\nu_A + eJ_{AX}/2) & k_{BA} & & \\ k_{AB} & -k_{BA} - k_{BC} - R_2^*{}_B + 2\pi i(\nu_B + eJ_{BX}/2) & k_{CB} & \\ & k_{BC} & -k_{CB} - k_{CD} - R_2^*{}_C + 2\pi i(\nu_C + eJ_{CX}/2) & k_{DC} \\ k_{AD} & & k_{CD} & -k_{DC} - k_{DA} - R_2^*{}_D + 2\pi i(\nu_D + eJ_{DX}/2) \end{bmatrix}$$

p_D, p_A, p_B, p_C, p_D) at $t = 0$. These populations p of the four species are related to the equilibrium constants of Scheme 1 by

$$K_1 = p_B/p_A \quad (2)$$

$$K_2 = p_D/(p_A E) \quad (3)$$

$$K_3 = p_C/(p_B E) \quad (4)$$

$$K_4 = p_C/p_D \quad (5)$$

In the matrix **M**, k are the rate constants (see Scheme 1), ν are the chemical shifts, R_2^* is the apparent transverse relaxation rate in the absence of chemical exchange, and i is the imaginary number. The subscripts indicate the sites A, B, C, and D. The coupling constants J represent the coupling between the A part and the correspoding X part of an AX spin system. In the line shape analyses of the alanyl methyl protons and the amide protons, this is the vicinal coupling to the corresponding C^α proton. For the line shape analyses of the signals of the ring protons of the 4-nitroanilide residue, which is an AA′BB′ spin system, the same matrix was used because it appears almost like an AX spin system even without exchange. This approximation is possible since the scalar couplings between A and A′ and A and B′ are small and consequently have nearly no influence on the line shapes of signals with chemical exchange.

An in-house FORTRAN program based on programs of Binsch (Kleier & Binsch, 1969) was used to simulate the line shapes. An arbitrary number of spectra can be simulated in a single run, and multiple parameters can be automatically varied to obtain the best agreement between the experimental and calculated line shapes as judged by means of the error square sum, the R factor

$$R \text{ factor} = \sqrt{\sum[y(i) - f(i)]/\sum y(i)^2} \quad (6)$$

where $y(i)$ and $f(i)$ are experimental and calculated data points, respectively. The Marquardt−Levenberg algorithm (Marquardt, 1964) was used in the nonlinear least-squares fitting procedure.

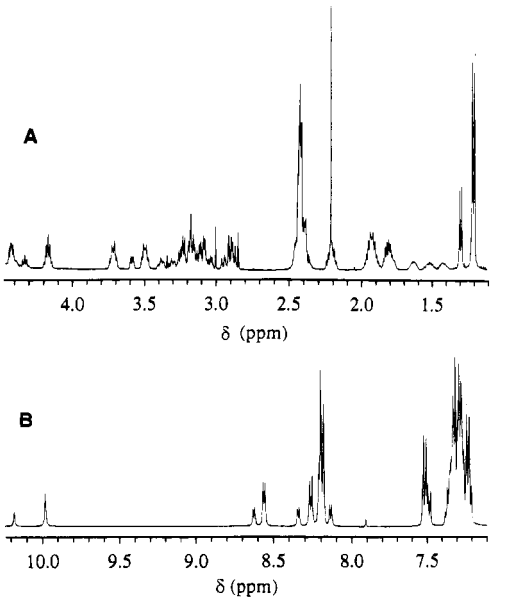

FIGURE 1: 500 MHz ^{1}H NMR spectrum of 5 mM Suc-Ala-Phe-Pro-Phe-(4-)NA in 10 mM phosphate buffer, pH 6.0, at 10 °C: (A) aliphatic protons; (B) aromatic and amide protons. The singlets at 2.2, 2.83, 3.0, and 7.91 ppm are impurities. The assignments of the signals are summarized in Table 1.

RESULTS

For a number of protons of Suc-Ala-Phe-Pro-Phe-(4-)NA, distinct signals occur for the *trans* and *cis* isomers in the 1D ^{1}H NMR spectrum (Figure 1). This shows that the *cis/trans* interconversion is slow on the NMR time scale. The assignments of the signals in Figure 1 are summarized in Table 1.

The *cis/trans* ratio was determined from the ratio of the integrals to 26:74, which is in good agreement with the value of 24% *cis* obtained from the isomer-specific proteolysis.

Table 1: ^{1}H NMR Chemical Shifts of the *Cis* and the *Trans* Isomer of Suc-Ala-Phe-Pro-Phe-(4-)NA at 10 °C[a]

	chemical shifts (ppm)					
residue[b]	NH	C^α	C^β	C^γ	C^δ	other
Suc^1_t						2.43 (2,3H)
Suc^1_c						2.40 (2,3H)
Ala^2_t	8.21	4.18	1.21			
Ala^2_c	8.13	4.33	1.30			
Phe^3_t	8.26	*c*	3.18, 3.22			7.20−7.40 (ring)
Phe^3_c	8.34	*c*	3.18, 3.38			
Pro^4_t		4.42	1.81, 2.21	1.94, 1.94	3.50, 3.71	
Pro^4_c		4.50	1.42, 1.62	1.52, 1.78	3.30, 3.60	
Phe^5_t	8.57	4.52	2.90, 3.10			7.20−7.40 (ring)
Phe^5_c	8.62	*c*	2.95, 3.05			
$(4\text{-})NA^6_t$	9.99					7.52 (2,6H)
						8.20 (3,5H)
$(4\text{-})NA^6_c$	10.18					7.48 (2,6H)
						8.20 (3,5H)

[a] The chemical shifts are referred to the H2O signal at 4.92 ppm. [b] The subscripts c and t denote the *cis* and *trans* isomer. [c] The signals are under the water signal.

Scheme 1: The Four-Site Exchange Model for the Cyp18-Catalyzed *Cis/Trans* Isomerization of Suc-Ala-Phe-Pro-Phe-(4-)NA[a]

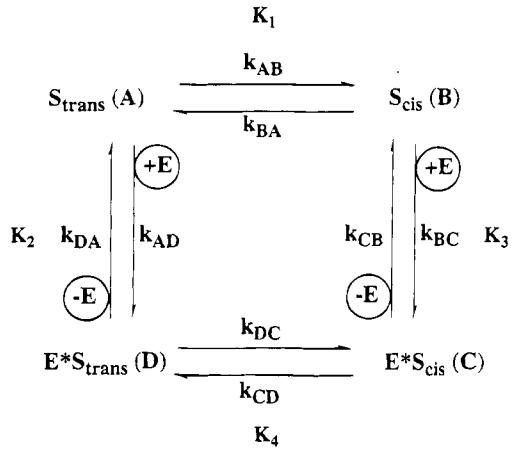

[a] K_1 and K_4 are the equilibrium constants $[A_{cis}]/[S_{trans}]$ and $[E^*S_{cis}]/[E^*S_{trans}]$, K_2 and K_3 the association constants, E represents Cyp18, and the symbols A and B mark the free isomers and C and D the enzyme-bound species. The individual microscopic rate constants k are marked with the corresponding subscripts.

For complete line shape analyses, parts of the spectra with well-separated *cis/trans* pairs and simple spin coupling patterns were selected. These prerequisites are fulfilled for the alanyl methyl protons and several amide protons.

In principle, minimally four species have to be considered for the catalytic cycle of prolyl *cis/trans* isomerization: the free *cis* and *trans* isomers as well as two Michaelis complexes. The simplest reaction model including all species is depicted in Scheme 1. It gives rise to a four-site exchange in a dynamic NMR experiment.

Under certain simplifying assumptions, the four-site exchange may be reduced into either a three- or two-site exchange. An apparent two-site exchange could only be envisioned if two conditions coincide, extremely fast on and off rates and identical chemical shifts in the free and enzyme-bound states of the peptide. This model we could rule out (Hübner et al., 1991), which indicates that the chemical shifts of the enzyme-bound and free peptide are different at least for either the *cis* or the *trans* isomer. We have now found it impossible to get a satisfying agreement between experimental spectra and theoretical spectra calculated according to a three-site model that assumed a common Michaelis complex for *cis* and *trans* substrate.

In order to find the best conditions to determine all the parameters describing the four-site exchange model we initially performed an experiment where the substrate concentration was varied in the presence of a constant cyclophilin concentration (Figure 2). These spectra show that the line shape is sensitive to the substrate concentration within the used range. This proves that even the lowest substrate concentration of 340 μM is at or above K_M, in agreement with a value of 100 μM for *cis*-Suc-Ala-Phe-Pro-Phe-(4-)NA by the improved PPIase assay (Kofron et al., 1991).

In our reaction scheme there is no K_M value, but the association constants for the *cis* and *trans* isomer, K_2 and K_3. In the line shape calculations, only rate constants are used with $K_2 = k_{AD}/k_{DA}$ and $K_3 = k_{BC}/k_{CB}$. Only for very fast on and off rates will the expression $K_2 = 1/K_{M(trans)}$ be fulfilled. By using the reaction scheme shown in Scheme 1 it is possible to obtain rate and association constants without

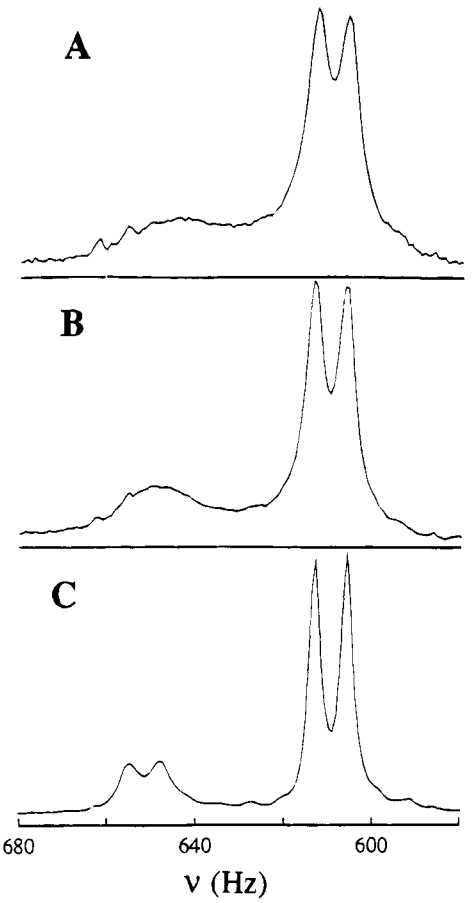

FIGURE 2: Dependence on peptide concentration of the line shape at constant Cyp18 concentration. Expansion of Figure 1 showing the *cis* and *trans* signals of the alanyl methyl protons in the presence of 30 μM Cyp18 and peptide concentrations of (A) 340, (B) 650, and (C) 1800 μM.

the assumption of fast exchange. We have therefore fitted theoretical line shapes calculated according to the matrix given in Materials and Methods to the experimental data.

In addition to the variables that could be determined from the spectrum of peptide in the absence of Cyp18 (ν_A, ν_B, J_{AX} and J_{BX}, K_1) and the constants measured by isomer-specific proteolysis (k_{AB}, k_{BA}), the matrix contains several variables that had to be determined by line shape analyses of the NMR spectra taken at various peptide and enzyme concentrations. These variables can be grouped into two categories: (i) NMR-related parameters—apparent relaxation rates, coupling constants, and chemical shifts; and (ii) kinetic parameters.

Referring to (i) the apparent relaxation rates for the free peptide resonances, $R_2{}^*{}_A$ and $R_2{}^*{}_B$, can be obtained directly for a sample without enzyme from the line widths of the signals (eq 7), since the exchange is too slow to affect the NMR line shape. For samples with enzyme present, a singlet at 3.0 ppm, representing residual solvent from the peptide synthesis which is not affected by enzyme, has been used as a line shape reference to monitor variations in homogeneity, and the relaxation rates for the free peptide resonances, $R_2{}^{*\prime}{}_A$ and $R_2{}^{*\prime}{}_B$, are given by eq 8. In eqs 7 and 8, $\Delta\nu^0{}_{1/2}$,

$$R_2 = \pi\Delta\nu^0{}_{1/2} \tag{7}$$

$$R_2{}^{*\prime} = R_2{}^* + \pi(\Delta\nu^{ref}{}_{1/2} - \Delta\nu^{ref0}{}_{1/2}) \tag{8}$$

Table 2: Selected Solutions Derived from the Line Shape Analyses by Varying the Starting Parameters of Iteration for the Signals of the Ala[2] Protons[a]

K_3[b] (M^{-1})	3000	5000	12000	13000	14000	15000	16000	18000	24000	30000
K_2[c] (M^{-1})	1930	3830	2950	3910	3770	3520	3850	4220	4960	4000
K_4	0.53	0.44	1.38	1.13	1.26	1.45	1.41	1.45	1.63	2.55
k_{BC} ($10^7 s^{-1} M^{-1}$)	1.4	2.1	2.4	2.8	2.7	2.7	2.7	3.3	3.7	4.3
k_{CB}[c] (s^{-1})	4520	4220	1980	2180	1930	1470	1710	1840	1560	1450
k_{CD}[c] (s^{-1})	2880	2140	1090	1065	1010	1015	1400	1280	1540	1360
k_{DC} (s^{-1})	1520	950	1500	1200	1280	1470	1970	1860	2510	3470
k_{DA}[c] (s^{-1})	3620	3800	4330	4840	5340	5110	2260	2310	1450	1480
k_{AD} ($10^7 s^{-1} M^{-1}$)	0.7	1.45	1.3	1.9	2.0	1.8	0.9	1.0	0.7	0.6
$\Delta\delta_{trans}$[c] (ppm)	0.05	0.05	0.1	0.1	0.1	0.1	0.1	0.2	0.3	0.7
$\Delta\delta_{cis}$[c] (ppm)	0.9	0.7	0.5	0.4	0.4	0.3	0.3	0.25	0.2	0.15
$k_{cat}/K_M(cis)$ ($s^{-1} \mu M^{-1}$)	4.2	6.1	6.9	7.9	8.0	8.2	8.3	9.2	10	9.7

[a] The values k_{AB}, k_{BA}, and K_1 were determined from the spectrum of the peptide in the absence of Cyp18 or from the protease-coupled PPIase assay to 0.0018 s^{-1}, 0.0053 s^{-1}, and 0.34, respectively, and kept constant in the iteration. [b] The values of K_3 were kept constant for the respective iteration. [c] Determined iteratively by line shape analyses; all other parameters were calculated from either the mass action law or with eqs 9−13.

$\Delta\nu^{ref}{}_{1/2}$, and $\Delta\nu^{ref0}{}_{1/2}$ denote the line width at half-height for the actual signal in the absence of enzyme and for the reference in the presence and absence of enzyme, respectively.

The relaxation rates of the nuclei when the peptide is enzyme-bound ($R_2{}^*{}_C$ and $R_2{}^*{}_D$) are not directly available. However, the enzyme/peptide ratio is at most 1:20, and therefore, these relaxation rates are not supposed to influence the shape of the observed spectrum significantly. In fact, in test calculations with $R_2{}^*$ values from 12.5 to 50 s^{-1} (resulting for line widths from 4 to 16 Hz) for the enzyme-bound peptide, no effect could be detected. A value of 20 s^{-1} was therefore used throughout.

The vicinal coupling constants of the cyclophilin-bound isomers cannot be measured. Also, these values have no influence of the line shape and therefore the simplification $J_{AX} = J_{DX}$ and $J_{BX} = J_{CX}$ was used. The chemical shifts of the two enzyme-bound substrate species, ν_C and ν_D, were determined iteratively.

Referring to (ii) as depicted by Scheme 1, there are eight rate constants describing a four-site exchange. The rate constants for the uncatalyzed reaction, k_{AB} and k_{BA}, were determined as described above. From the remaining six rate constants, only five are independent, which were determined by iteration. The sixth one can be calculated on the basis of the principle of microscopic reversibility for a system at equilibrium.

The line shape analyses were performed on the signals of the alanyl methyl protons, the amide protons of Phe[3], Phe[5], and (4-)NA[6], and the ring protons 2 and 6 of (4-)NA[6]. Initially the methyl resonances were used, and we first tried to fit the data allowing the chemical shifts to vary freely but assuming fast exchange in the binding of the peptide to the enzyme (k_{CB} and $k_{DA} \gg k_{DC}$ and k_{CD}). Even though every single spectrum could be well simulated with this assumption, it was impossible to simulate all spectra with a single set of parameters. Therefore it was necessary to vary also the on and off rates in addition to the association constants. In this way it was possible to obtain a very good agreement between experimental and calculated spectra, as shown in Figure 3. One has, however, to keep in mind that the best fit obtained by variation of many parameters, as in this case, does not necessarily result in a unique solution. Different starting values for various parameters result in somewhat different sets of final parameters and with very similar R factors. Some of the unknown parameters are restricted: The upper value for the on rates of substrate to Cyp18 is diffusion limited, about 10^8 M^{-1} s^{-1} for small molecules in water (Hammes & Schimmel, 1970; Benner, 1989). Furthermore, the chemical shifts of the nuclei in the enzyme-bound peptide are limited to the following ranges: 0−2 ppm for the alanyl methyl group, 7−11 ppm for the amide protons, and 9−12 ppm for the anilide proton. Using these restrictions and a large number of spectra with different peptide and cyclophilin concentrations, the range of possible solutions was highly limited. Some uncertainity still remains because the chemical shifts of the two enzyme-bound species, ν_C and ν_D, are not well defined. These signals are not directly visible in the spectra, since the population of bound substrate is small compared to free substrate, their transverse relaxation rates are determined by the protein, and consequently their signals are broad. Furthermore, in this particular case, the exchange between free and bound substrate is intermediate on the NMR time scale, which makes it impossible to observe the signal for bound substrate. The chemical shifts ν_C and ν_D strongly correlate with the magnitude of the association constants K_3 and K_2, respectively. In order to define the space of possible solutions, K_3 was varied from 2×10^3 to 4×10^4 M^{-1} in steps of 500 M^{-1} (Table 2).

Allowed values for K_2 were found to be 2×10^3 to 6×10^3 M^{-1} and for K_3, 3×10^3−3×10^4 M^{-1}. In all cases, K_3 is larger than K_2. In the described range of solutions, small K_3 values correlate with a large difference in chemical shift between bound and free *cis* isomer and a small difference between bound and free *trans* isomer. Correspondingly large K_3 values correlate with a small difference in chemical shift between bound and free *cis* isomer and a large difference between bound and free *trans* isomer. For intermediate values of K_2 and K_3, the differences in the chemical shift between bound and free substrate are similar for both isomers. The R factor (eq 6) as well as visual inspection were used to evaluate the agreement of the simulated with the experimental spectra.

With the described line shape analyses, the space of solutions could be strongly narrowed, but a unique solution could not be found due to the above explained uncertainity in the chemical shifts of the bound peptide isomers.

However, by combining the results from the line shape analyses with the k_{cat}/K_M value for the catalyzed *cis* → *trans* isomerization obtained from the protease-coupled PPIase assay, a unique solution can be selected, since these kinetics are of course independent of NMR parameters. The ratio k_{cat}/K_M of the PPIase catalysis is a complex expression composed of the microscopic rate constants depicted in

Scheme 1. The individual reaction steps cannot be resolved with the protease coupled PPIase assay but can with line shape analyses. The minimal model of PPIase catalysis in Scheme 1 corresponds to a fully reversible enzyme reaction with the Michaelis complexes ES and EP. Using the corresponding equations (for $E_o \ll S_o$) (Segel, 1993):

$$v = \frac{\frac{\vec{V}}{K_{M(trans)}}[S_{o(trans)}] - \frac{\overleftarrow{V}}{K_{M(cis)}}[S_{o(cis)}]}{1 + \frac{[S_{o(trans)}]}{K_{M(trans)}} + \frac{[S_{o(cis)}]}{K_{M(cis)}}} \quad (9)$$

$$K_M(trans) = \frac{k_{CB}k_{DA} + k_{CB}k_{DC} + k_{CD}k_{DA}}{k_{AD}(k_{CB} + k_{CD} + k_{DC})} \quad (10)$$

$$K_M(cis) = \frac{k_{CB}k_{DA} + k_{CB}k_{DC} + k_{CD}k_{DA}}{k_{BC}(k_{CD} + k_{DC} + k_{DA})} \quad (11)$$

$$\vec{V} = \frac{k_{CB}k_{DC}[E_o]}{k_{CB} + k_{CD} + k_{DC}} = k_{cat(trans)}[E_o] \quad (12)$$

$$\overleftarrow{V} = \frac{k_{CD}k_{DA}[E_o]}{k_{CD} + k_{DC} + k_{DA}} = k_{cat(cis)}[E_o] \quad (13)$$

k_{cat} and K_M for the *cis* → *trans* as well as for the *trans* → *cis* isomerization can be calculated from the microscopic rate constants derived from the line shape analyses. In eq 9 the reaction rate v describes the change of concentration of the *trans* isomer with time and equals zero at equilibrium. The symbols $\vec{V}$ and $\overleftarrow{V}$ represent the maximal velocities of the forward (*trans* → *cis*) and reverse (*cis* → *trans*) reactions, respectively.

Scheme 1 is also valid for the protease-coupled PPIase assay except that the reactions *trans* → *cis* (A → B) and the binding of the *trans* isomer to Cyp18 (A → D) do not occur due to the coupled fast proteolytic cleavage of the *trans* isomer. All individual reactions that contribute to k_{cat} and K_M of the *cis* isomer are identical in both experiments and can therefore be compared directly. Thus, all sets of constants resulting from line shape analyses could be used to calculate $k_{cat}/K_M(cis)$ from eqs 11 and 13. Only one of the different sets of solutions agreed with the $k_{cat}/K_M(cis)$ value of 8.2 μM^{-1} s^{-1} obtained by the protease-coupled assay. All other possible solutions gave values significantly different from this value (see Table 2). In addition to the $k_{cat}/K_M(cis)$ value, the individual steady state constants k_{cat} and K_M calculated from eqs 11 and 13 also were in good accordance with the values measured with the improved PPIase assay (Kofron et al., 1991).

The finally determined microscopic and steady state constants for the four-site exchange model of PPIase catalysis are summarized in Table 3. The corresponding simulated line shapes together with their experimental spectra are shown in Figure 3. In contrast to a two-site model (Hübner et al., 1991), a four-site exchange model fits the experimental spectra very well.

To further support these findings, the line shape analyses were also performed for the signals of the amide protons of Phe[3], Phe[5], and (4-)NA and for the ring protons 2 and 6 of (4-)NA. For all signals, the calculated microscopic rate constants reside within the error range given in Table 3. The line shape analyses of these signals further limited the range of possible solutions obtained from NMR alone. The changes in chemical shift of these protons due to substrate binding to Cyp18 are summarized in Table 4.

It is obvious that for residues N-terminal to proline these chemical shift differences are similar for both isomers but

Table 3: Microscopic and Steady State Constants for the Four-Site Exchange Model for Cyp18-Catalyzed *Cis/Trans* Isomerization in Suc-Ala-Phe-Pro-Phe-(4-)NA

Microscopic Constants	
k_{AB}[a] (s^{-1}) 0.00180 ± 0.00007	k_{DA}[b] (s^{-1}) 5110 ± 300
k_{BA}[a] (s^{-1}) 0.0053 ± 0.0002	k_{AD} (s^{-1} M^{-1}) (1.8 ± 0.3) × 10^7
k_{BC} (s^{-1} M^{-1}) (2.7 ± 0.4) × 10^7	K_1[a] 0.34 ± 0.01
k_{CB}[b] (s^{-1}) 1800 ± 100	K_2[b] (M^{-1}) 3520 ± 500
k_{CD}[b] (s^{-1}) 1015 ± 150	K_3[b] (M^{-1}) 15000 ± 1500 M
k_{DC} (s^{-1}) 1470 ± 200	K_4 1.45 ± 0.2
Steady State Constants	
$K_M(trans)$ (μM) 220 ± 40	$k_{cat}(cis)$ (s^{-1}) 680 ± 100
$K_M(cis)$ (μM) 80 ± 20	$k_{cat}/K_M(trans)$ (s^{-1} μM^{-1}) 2.8 ± 0.2
$k_{cat}(trans)$ (s^{-1}) 620 ± 100	$k_{cat}/K_M(cis)$[a] (s^{-1} μM^{-1}) 8.2 ± 0.2

[a] The values k_{AB}, k_{BA}, and K_1 were determined from the spectrum of the peptide in the absence of Cyp18 or from the protease-coupled PPIase assay to 0.0018 s^{-1}, 0.0053 s^{-1}, and 0.34, respectively, and kept constant in the iteration. [b] Determined iteratively by line shape analyses; all other parameters were calculated from either the mass action law or with eqs 9–13.

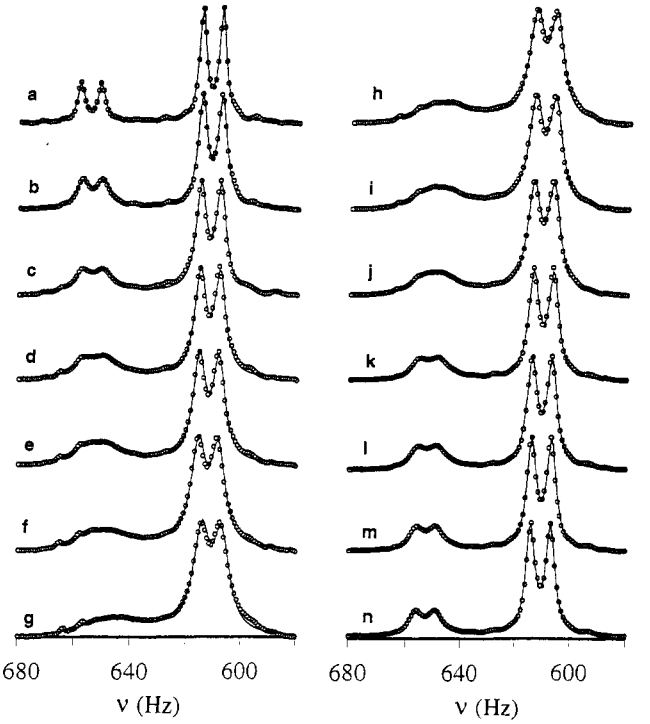

FIGURE 3: Simulation of the Cyp18 catalysis according to a four-site exchange model. Experimental data (O) [alanyl methyl protons of Suc-Ala-Phe-Pro-Phe-(4-)NA in 10 mM phosphate buffer, pH 6.0, at 10 °C] are superimposed by the simulated line shapes according to the matrix given in Materials and Methods using the parameters of Table 3. Left column: addition of increasing amounts of Cyp18 [E_o] to the peptide solution [S_o] (a) 400 μM [S_o], 0 μM [E_o]; (b) 390 μM [S_o], 2.16 μM [E_o]; (c) 380 μM [S_o], 4.22 μM [E_o]; (d) 370 μM [S_o], 6.2 μM [E_o]; (e) 365 μM [S_o], 8.15 μM [E_o]; (f) 350 μM [S_o], 13.6 μM [E_o]; (g) 340 μM [S_o], 15.5 μM [E_o]. Right column: addition of increasing amounts of peptide [S_o] to solution g. (h) 500 μM [S_o], 15.25 μM [E_o]; (i) 650 μM [S_o], 15 μM [E_o]; (j) 800 μM [S_o], 14.5 μM [E_o]; (k) 1320 μM [S_o], 14.2 μM [E_o]; (l) 1470 μM [S_o], 14.07 μM [E_o]; (m) 1840 μM [S_o], 14 μM [E_o]; (n) 2300 μM [S_o], 13.8 μM [E_o]. The small signals at 660 Hz in spectra c–j are protons of residual tricine buffer in the Cyp18 stock solution.

Table 4: Differences of Chemical Shifts of Selected Protons of Suc-Ala-Phe-Pro-Phe-(-4)NA between the Free and Cyp18-Bound Peptide

	$\Delta\delta = \delta_{free} - \delta_{bound}$ (ppm)	
residue	*trans* isomer	*cis* isomer
Ala^2 C$^\beta$H$_3$	+0.1 ± 0.2	+0.3 ± 0.2
Phe^3 NH	+0.1 ± 0.2	−0.2 ± 0.3
Phe^5 NH	-0.1 ± 0.2	−1.8 ± 0.2
(4-)NA^6 NH	+0.4 ± 0.2	−0.8 ± 0.4
(4-)NA^6 2,6H	+0.0 ± 0.1	+0.5 ± 0.2

not for the residues C-terminal to proline. The most striking fact is the 1.8 ppm downfield shift of the amide proton signal of Phe^5(*cis*). The interpretation will be given in the Discussion.

DISCUSSION

The aim of this work was to elaborate a minimal reaction mechanism for Cyp18-catalyzed prolyl *cis/trans* isomerization for an oligopeptide and also to determine the complete set of microscopic rate constants for the different steps contributing to enzyme catalysis. Dynamic NMR spectroscopy was found to be a powerful method to characterize the PPIase-catalyzed *cis/trans* isomerization under equilibrium conditions. Previously 2D exchange spectroscopy (Justice et al., 1990; Kern et al., 1993) and saturation transfer (Hsu et al., 1990; London et al., 1990; Videen et al., 1994) were used to detect PPIase catalysis on nonchromogenic substrates. Both techniques allow only the determination of exchange rates which represent a sum of several reaction steps and thus have the same limitations as the photometric assays (Kofron et al., 1991; Garcia-Echeverria et al., 1992, 1993). In contrast, the line shape analyses used in this work allowed the kinetic characterization of all of the individual reactions involved in the minimal reaction sequence for PPIase catalysis. It therefore provides access to the molecular aspects of the enzyme mechanism. The reason that the line shape technique is sensitive not only to the *cis/trans* isomerization rate of bound peptide but also to the on/off rates is, first, that the isomerization rates and the off rates are of comparable magnitude and, second, that the chemical shifts are different for the free and enzyme-bound peptide. Four species are required to explain the isomerization kinetics of Suc-Ala-Phe-Pro-Phe-(4-)NA in the presence of Cyp18. The line shapes of the experimental data could be fitted to a four-site exchange model over a wide range of enzyme and substrate concentrations. The three-site exchange model did not fully describe the experimental data. The four-site model would be reduced to a three-site model if only one enzyme-bound species exists. This would likely occur by docking the prolyl peptide bond to the enzyme in an approximate transition state structure with a proline ring arranged perpendicularly to the carbonyl group. Only the line shapes of the alanyl methyl protons could be simulated according to a three-site exchange. In this case, the chemical shifts of the enzyme-bound *cis* and *trans* isomer are similar, which makes it impossible to distinguish between a three- and a four-site exchange. For all other signals the chemical shifts of the *cis* and the *trans* isomers bound to the enzyme are different. Here the data could not be fitted according to a three-site exchange model.

For the first time we determined the microscopic rate constants for all individual steps in the Cyp18-catalyzed *cis/trans* isomerization according to a four-site exchange model. Our data demonstrate that the rates of formation of the Michaelis complexes with the *cis* and *trans* peptide are significantly lower than the diffusion limit, and the dissociations of the corresponding ES complexes are similar in rate to the isomerization step on the enzyme. Consequently the steady state parameters k_{cat} and K_M are complex parameters and cannot be attributed to a single step in the reaction cycle but depend on all microscopic rate constants in the exchange model. Thus, it becomes obvious that the observed secondary β-deuterium isotopic effects on the apparent k_{cat}/K_M values (Fischer et al., 1989b; Harrison & Stein, 1990) cannot be used for a molecular interpretation with regard to the enzyme mechanism, since the individual steps might contribute conversely to the measured effects. Mechanistic considerations based on the second-order rate constants may suffer from the same reason (Harrison & Stein, 1992).

Scheme 2

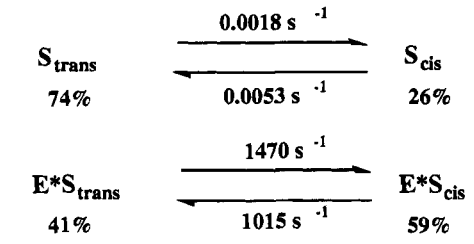

In Scheme 2, the microscopic rate constants of *cis/trans* isomerization in the enzyme-bound substrate state and in free solution are compared. The acceleration factor is 8.2×10^5 for the *trans* → *cis* isomerization and 1.9×10^5 for the reverse reaction. It becomes apparent that the efficiency of Cyp18 to accelerate *cis/trans* isomerization is slightly underestimated, when k_{cat} is compared to the nonenzymic rate constants (Table 3). Thus, the acceleration factor of Cyp18, as calculated from k_{cat} by Kofron for a more favorable substrate, may be higher than reported there (Kofron et al., 1991). This shows that the catalytic proficiency (Radzicka & Wolfenden, 1995) of Cyp18 is indeed not very high. However for enzymes, catalyzing naturally fast reactions, the absolute value of rate constants may be more important than the acceleration factor itself. In consideration of this, Cyp18 belongs to the well-developed enzymes.

Scheme 2 also shows that the *cis/trans* equilibrium is shifted toward the *cis* isomer by binding of the peptide to Cyp18. Thus, the enzyme provides an environment that stabilizes the *cis* conformer by 3.4 kJ mol^{-1}. The exclusive detection of the *cis* prolyl peptide bonds in the X-ray structures of peptides bound to human Cyp18 (Kallen & Walkinshaw, 1992; Ke et al., 1993) could be explained by this finding.

Kakalis and Armitage (1994) concluded from TRNOE experiments that the cyclophilin-bound conformation of Suc-Ala-Ala-Pro-Phe-(4-)NA in solution has a *cis*-like prolyl peptide bond. However, the authors suggest a model with only one unique enzyme-bound state. The method of TRNOE cannot distinguish between a three-site and a four-site model since *cis/trans* isomerization on the enzyme is too fast. Our results clearly show the existence of two different Michaelis complexes. Therefore the conformation of the peptide determined by TRNOE represents an average conformation between the bound *cis* and *trans* isomers and is determined by the ratio of the two isomers in the bound state. The *cis*-like conformation observed by Kakalis (Kaka-

lis & Armitage, 1994) is well explained by the stronger binding of the *cis* isomer.

Burbaum et al. suggested that for an catalytically optimized enzyme the internal equilibrium constant K_{int} = [ES]/[EP] depends on how close to equilibrium the enzyme maintains its reaction under physiological conditions (Burbaum et al., 1989). Even if the equilibrium constant in the absence of enzyme (K_{eq}) deviates strongly from unity, operation near equilibrium is predicted to have a K_{int} value near unity. In contrast to that, enzymes that operate far away from equilibrium show values of K_{int} that differ from unity in the direction of the catalyzed reaction. The internal equilibrium constant $[ES_{cis}]/[ES_{trans}]$ of 1.45 for Cyp18 thus points to a biological function of Cyp18 for the catalysis of the *cis/trans* isomerization in a reversible manner. Reversible *cis/trans* isomerization is realized in the native state isomerization of proteins (Evans et al., 1987; Higgins et al., 1988; Chazin et al., 1989). Catalysis by PPIases of this event could not be found, so far. An attempt to detect Cyp18 catalysis of such a native state isomerization in Calbindin D9k *in vitro* remained unsuccessful (Kördel et al. 1990). In cellular protein folding, *cis/trans* isomerization is followed by the irreversible formation of the native polypeptide chain which may be rate-limiting in the presence of PPIases. Even in this case, rapid equilibration of the *cis/trans* isomers in the coupled reaction may occur. Indeed both *trans* → *cis* isomerization (Wetlaufer, 1985; Kruse et al. 1995) and *cis* → *trans* isomerization (Engel & Pockrop, 1991) was postulated and observed in *de novo* polypeptide folding in the cell.

An important aspect of the shift of the *cis/trans* equilibrium in the Michaelis complexes of Cyp18 toward the *cis* conformation resides in the high intracellular enzyme concentration of approximately 4 μM in human erythrocytes, for example (Agarwal et al., 1987). Since a potential substrate may be found in a much lower amount in the cell, an isomer-specific extraction of the *cis* isomer could occur. This intrinsically leads to an intracellular pool of protein-bound *cis* prolyl conformers which are disfavored relative to the *trans* isomer free in solution. According to the values depicted in Table 3, the rapid dissociation of the *cis* isomer from the enzyme then ensures its availability for fast recognition processes.

Besides all microscopic rate constants, the k_{cat} and K_M values for the *cis* and for the first time also for the *trans* isomer could be determined. The steady state constants for the *trans* → *cis* reaction are of special interest, since this interconversion is often the rate-limiting step in protein folding. While the k_{cat} values for both isomers are comparable, the K_M for the *trans* isomer is 3 times larger than that for the *cis* isomer.

Nothing is so far known about the differences in the spatial proximity of the two isomers on the enzyme, because X-ray stuctures of Cyp18 in complex with *trans* isomers are not available and because the TRNOE experiments provide only information about the peptide conformation in the enzyme-bound state, but nothing about the local protein environment of the bound species. With line shape analyses we determined the changes in chemical shift of different protons caused by binding to the protein ($\Delta\delta = \delta_{free} - \delta_{bound}$). The $\Delta\delta$ values of the investigated signals of the residues N-terminal to proline are similar for both isomers. This suggests that in both isomeric forms these residues bind in a similar spatial environment to the protein. However, the $\Delta\delta$ values for protons in residues C-terminal to proline are larger for the *cis* isomer than for the *trans* isomer, suggesting a different environment for these residues in their complexes with the protein. Ke et al. (1993) already speculated that either the peptide residues C-terminal or those N-terminal to proline should be fixed on Cyp18, whereas the remaining part of the peptide could rotate during catalysis. From their data it was not possible to decide which part of the peptide would remain fixed and which one would rotate, because Ala-Pro was used as a probe. Besides lack of a C-terminal part, the dipeptide does not represent a substrate for Cyp18 but a competitive inhibitor (Fischer et al., 1994). Our results suggest that the peptide chain C-terminal to proline might be rotated. The largest change in chemical shift by binding of the substrate to Cyp18 was determined for the NH resonance of Phe^5 in the *cis* isomer. This signal is shifted 1.8 ppm downfield, which may be due to the formation of a hydrogen bond from the peptide bond to either a suitable group of enzymes or an enzyme-bound water molecule. No similar effect was found for the *trans* isomer. Deshielding of the NH proton by adjacent aromatic residues of the protein may be of minor importance for the shift. In the enzyme-bound *cis* isomer, Phe^{60} represents the closest aromatic residue. The ring atoms of the Phe^{60} side chain are still quite distant (>5 Å) to the NH group, and the aromatic ring is out of the NH bond plane (H. Ke, personal communication). The hydrogen bond could explain why the *cis* isomer binds tighter than the *trans* isomer. The ratio of K_3/K_2 = 4.3 corresponds to a difference in free enery of 3.4 kJ/mol at 10 °C, which is well within the difference between a strong and a weak hydrogen bond. However, we also have to consider that the NH of Phe^5 of the trans isomer may be solvated in the enzyme-bound state and there is little, if any, to gain in changing hydrogen bond from water to a hydrogen bond receptor in the protein. Thus, with some caution, this work gives also a tentative explanation of the preferred binding of the *cis* isomer in addition to a detailed discription of the enzyme kinetics for Cyp18.

ACKNOWLEDGMENT

We thank F. X. Schmid for helpful discussions and critically reading the manuscript and Hengming Ke for providing unpublished data about a cyclophilin/substrate complex.

REFERENCES

Agarwal, R. P., Threatte, G. A., & McPherson, R. A. (1987) *Clin. Chem. 33*, 481−485.
Bächinger, H. P. (1987) *J. Biol. Chem. 262*, 17144−17148.
Baker, E. K., Colley, N. J., & Zuker, C. S. (1994) *EMBO J. 13*, 4886−4895.
Benner, S. A. (1989) *Chem. Rev. 89*, 789−806.
Binsch, G. (1969) *J. Am. Chem. Soc. 91*, 1304−1306.
Burbaum, J. J., Raines, R. T., Albery, W. J., & Knowles, J. R. (1989) *Biochemistry 28*, 9293−9323.
Cardenas, M. E., Hemenway, C., Muir, R. S., Ye, R., Fiorentino, D., & Heitman, J. (1994) *EMBO J. 13*, 5944−5957.
Chazin, W. J., Kördel, J., Drakenberg, T., Thulin, E., Brodin, P., Grundström, T., & Forsen, S. (1989) *Proc. Natl. Acad. Sci. U.S.A. 86*, 2195−2198.
Engel, J., & Prockop, D. J. (1991) *Annu. Rev. Biophys. Chem. 20*, 137−152.
Evans, P. A., Dobson, C. M., Kautz, R. A., Hatfull, G., & Fox, R. O. (1987) *Nature 329*, 266−268.
Fischer, G. (1994) *Angew. Chem. 106*, 1479−1501.
Fischer, G., Bang, H., & Mech, C. (1984) *Biomed. Biochim. Acta 43*, 1101−1111.
Fischer, G., Wittmann, L. B., Lang, K., Kiefhaber, T., & Schmid, F. X. (1989a) *Nature 337*, 476−478.

Fischer, G., Berger, E., & Bang, H. (1989b) *FEBS Lett. 250*, 267−270.
Fischer, G., Wöllner, S., Schönbrunner, R., & Scherer, G. (1994) *Proc. 5th Akabori Conf.* 142−145.
Franke, E. K., Yuan, H. E. H., & Luban, J. (1994) *Nature 372*, 359−362.
Fransson, C., Freskgard, P. O., Herbertsson, H., Johansson, A., Jonasson, P., Martensson, L. G., Svensson, M., Jonsson, B. H., & Carlsson, U. (1992) *FEBS Lett. 296*, 90−94.
Friedman, J., Trahey, M., & Weissman, I. (1993) *Proc. Natl. Acad. Sci. U.S.A. 90*, 6815−6819.
Garcia-Echeverria, C., Kofron, J. L., Kuzmic, P., Kishore, V., & Rich, D. H. (1992) *J. Am. Chem. Soc. 114*, 2758−2759.
Garcia-Echeverria, C., Kofron, J. L., Kuzmic, P., & Rich, D. H. (1993) *Biochem. Biophys. Res. Commun. 191*, 70−75.
Haendler, B., Hofer, R., & Hofer, W. E. (1987) *EMBO J. 6*, 947−951.
Hammes, G. G., & Schimmel, P. R. (1970) in *The Enzymes: Kinetics and Mechanism* 3rd ed. (Boyer, P. D., Ed.) Vol. 2, pp 67−114, Academic Press Inc., New York.
Handschumacher, R. E., Harding, M. W., Rice, J., & Drugge, R. J. (1984) *Science 226*, 544−546.
Harding, M. W., Galat, A., Uehling, D. E., & Schreiber, S. L. (1989) *Nature 341*, 758−760.
Harrison, R. K., & Stein, R. L. (1990) *Biochemistry 29*, 1684−1689.
Harrison, R. K., & Stein, R. L. (1992) *J. Am. Chem. Soc. 114*, 3464−3471.
Higgins, K. A., Craik, D. J., Hall, J. G., & Andrews, P. R. (1988) *Drug Des. Delivery 3*, 159−170.
Hsu, V. L., Handschumacher, R. E., & Armitage, I. M. (1990) *J. Am. Chem. Soc. 112*, 6745−6747.
Hübner, D., Drakenberg, T., Forsen, S., & Fischer, G. (1991) *FEBS Lett. 284*, 79−81.
Johnson, J. L., & Toft, D. O. (1994) *J. Biol. Chem. 269*, 24989−24993.
Justice, R. M., Kline, A. D., Sluka, J. P., Roeder, W. D., Rodgers, G. H., Roehm, N., & Mynderse, J. S. (1990) *Biochem. Biophys. Res. Commun. 171*, 445−450.
Kakalis, L. T., & Armitage, I. M. (1994) *Biochemistry 33*, 1495−1501.
Kallen, J., & Walkinshaw, M. D. (1992) *FEBS Lett. 300*, 286−290.
Ke, H., Mayrose, D., & Cao, W. (1993) *Proc. Natl. Acad. Sci. U.S.A. 90*, 3324−3328.
Kern, D., Drakenberg, T., Wikström, M., Forsen, S., Bang, H., & Fischer, G. (1993) *FEBS Lett. 323*, 198−202.
Kern, G., Kern, D., Schmid, F. X., & Fischer, G. (1995) *J. Biol. Chem. 270*, 740−745.
Kleier, A., & Binsch, G. (1969) *QCPE 140*.
Kofron, J. L., Kuzmic, P., Kishore, V., Colon, B. E., & Rich, D. H. (1991) *Biochemistry 30*, 6127−6134.
Kördel, J., Drakenberg, T., Forsen, S., & Thulin, E. (1990) *FEBS Lett. 263*, 27−30.
Kruse, M., Brunke, M., Escher A., Szalay, A. B., & Tropschug, M. (1995) *J. Biol. Chem. 270*, 2588−2594.
Lang, K., & Schmid, F. X. (1988) *Nature 331*, 453−455.
Lang, K., Schmid, F. X., & Fischer, G. (1987) *Nature 329*, 268−270.
Limbach, H. H. (1991) in *NMR-Basic Principles and Progress,* Vol. 23, Chapter 2, pp 63−164, Springer, Heidelberg.
Lin, L. N., Hasumi, H., & Brandts, J. F. (1988) *Biochim. Biophys. Acta 956*, 256−266.
Lodish, H. F., & Kong, N. (1991) *J. Biol. Chem. 266*, 14835−14838.
London, R. E., Davis, D. G., Vavrek, R. J., Stewart, J. M., & Handschumacher, R. E. (1990) *Biochemistry 29*, 10298−10302.
Marquardt, D. W. (1964) *QCPE 1428*.
Mücke, M., & Schmid, F. X. (1992) *Biochemistry 31*, 7848−7854.
Nadeau, K., Das, A., & Walsh, C. T. (1993) *J. Biol. Chem. 268*, 1479−1487.
Ondek, B., Hardy, R. W., Baker, E. K., Stamnes, M. A., Shieh, B. H., & Zuker, C. S. (1992) *J. Biol. Chem. 267*, 16460−16466.
Pfügl, G., Kallen, J., Schirmer, T., Jansonius, J. N., Zurini, M. G. M., & Walkinshaw, M. D. (1993) *Nature 361*, 91−94.
Radzicka, A., & Wolfenden, R. (1995) *Science 267*, 90−93.
Sack, R. A. (1958) *Mol. Phys. 1*, 163−168.
Schmid, F. X. (1992) in *Protein Folding* (Creighton, T. E., Ed.) pp 197−241, Freeman, New York.
Schmid, F. X., Mayr, L., Mücke, M., & Schönbrunner, R. (1993) *Adv. Protein Chem.* 44, 25−66.
Schönbrunner, E. R., Mayer, S., Tropschug, M., Fischer, G., Takahashi, N., & Schmid, F. X. (1991) *J. Biol. Chem.* 266, 3630−3635.
Segel, I. H. (1993) in *Enzyme Kinetics*, pp 29−34, John Wiley & Sons, Inc., New York.
Siekierka, J. J., Hung, S. H., Poe, M., Lin, C. S., & Sigal, N. H. (1989) *Nature 341*, 755−757.
Steinmann, B., Bruckner, P., & Superti-Furga, A. (1991) *J. Biol. Chem. 266*, 1299−1303.
Takahashi, N., Hayano, T., & Suzuki, M. (1989) *Nature 337*, 473−475.
Thall, M., Bukovsky, A., Kondo, E., Rosenwirth, B., Walsh, C. T., Sodroski, J. & Göttlinger, H. G. (1994) *Nature 372*, 363−365.
Videen, J. S., Stamnes, M. S., Hsu, V. L., & Goodman, M. (1994) *Biopolymers 34*, 171−175.
Wetlaufer, D. B. (1985) *Biopolymers 24*, 251−255.
Wüthrich, K., Spitzfaden, C., Memmert, K., Widmer, H., & Wider, G. (1991) *FEBS Lett. 285*, 237−247.

BI9510993